Bandcrossing of magnetic rotation bands in ^{137}Pr

Priyanka Agarwal,[1] Suresh Kumar,[1] Sukhjeet Singh,[2] Rishi Kumar Sinha,[3] Anukul Dhal,[3] S. Muralithar,[4] R. P. Singh,[4] N. Madhavan,[4] Rakesh Kumar,[4] R. K. Bhowmik,[4] S. S. Malik,[2] S. C. Pancholi,[4,5] L. Chaturvedi,[3,6] H. C. Jain,[7] and A. K. Jain[1]

[1]*Department of Physics, Indian Institute of Technology Roorkee, Roorkee 247667, India*
[2]*Department of Physics, Guru Nanak Dev University, Amritsar 143005, India*
[3]*Department of Physics, Banaras Hindu University, Varanasi 221005, India*
[4]*Inter-University Accelerator Center, New Delhi 110067, India*
[5]*Formerly at Department of Physics and Astrophysics, Delhi University, Delhi 110007, India*
[6]*Pandit Ravi Shankar Shukla University, Raipur 492010, India*
[7]*Tata Institute of Fundamental Research, Colaba, Mumbai 400 005, India*

(Received 22 August 2006; published 28 August 2007)

The odd mass nucleus ^{137}Pr has been studied to high spins in order to investigate the magnetic rotation phenomenon in mass 130 region using the ^{122}Sn(^{19}F, $4n$)^{137}Pr reaction at a beam energy of 80 MeV. A known $\Delta I = 1$ band has been extended to $J^{\pi} = 47/2^{-}$ with the addition of three new transitions. Directional Correlation of Oriented Nuclei (DCO) ratios and linear polarization measurements have been performed to assign the multipolarities of gamma transitions and the spins and parities of the energy levels in this band, now established as the $M1$ band. The combination of $M1$ transitions along with cross over $E2$ transitions have been observed in this band for the first time. The experimentally deduced $B(M1)/B(E2)$ ratios show a decrease with increasing spin after band-crossing suggesting magnetic rotation. TAC calculations for the 3qp: $\pi h_{11/2} \otimes \nu(h_{11/2})^{-2}$ configuration reproduce the experimental observations in the lower spin part of the $\Delta I = 1$ band and the 5qp: $\pi h_{11/2}(g_{7/2})^2 \otimes \nu(h_{11/2})^{-2}$ configuration reproduces the $\Delta I = 1$ band at higher spins; the crossing of the bands based on the two configuration leads to a back-bending also. Theoretical calculations also support a magnetic rotation nature for both the configurations.

DOI: 10.1103/PhysRevC.76.024321 PACS number(s): 21.60.Ev, 23.20.Lv, 27.60.+j

I. INTRODUCTION

Magnetic rotation (MR) phenomenon, observed more than a decade ago, represents a new kind of motion in nuclei [1,2]. It leads to rotation-like bands in nearly spherical nuclei, which have several peculiarities that are in sharp contrast to normal deformed (ND) and superdeformed (SD) rotational bands. For example, the MR bands show the presence of strong intraband magnetic dipole transitions whereas the crossover $E2$ transitions are either weak or almost absent—indicating that MR bands do not arise from the usual rotational motion due to anisotropic density distribution (a rotational top). They in fact arise due to an anisotropic current distribution and may be termed to be the consequence of a "magnetic top." Magnetic rotation is expected in nuclei near the magic numbers if high-j valence particles and valence holes are available and the nuclear deformation is small. Probably, the first MR band existing in the literature is the one in ^{81}Kr [3], though it has been shown to be so only recently [4]. Hübel *et al.* [1] and Clark *et al.* [5] in 1992 observed the first regular patterns of gamma rays in the spectra of ^{198,199}Pb nuclei. Amita *et al.* [6] had collected about 170 such bands which are spread into four mass regions, namely, $A = 195$, 135, 110, and 80; the number has now gone up to more than 200. The largest set of data on MR bands belongs to the Pb isotopes in the $A = 195$ mass region. Yet a considerable number of nuclides from other mass regions, where MR bands are expected, still remain unexplored.

Among the several observed features, the most identifying characteristic of MR bands is the decreasing $B(M1)$ with increasing rotational frequency. Frauendorf [2] proposed an innovative explanation for the MR bands in terms of a shears mechanism and presented the tilted axis cranking (TAC) model. A coupling of high-j proton particles (holes) in low (high) Ω orbital and high-j neutron holes (particles) in high (low) Ω orbital leads to a nearly perpendicular coupling of neutron and proton angular momentum vectors. The resultant angular momentum vector is, therefore, tilted with respect to one of the principal axes. Since the deformation is very weak, the usual rotational angular momentum vector is very small and the dynamics is mostly governed by the resultant of the neutron and proton vectors. The neutron and proton angular momentum vectors represent the two blades of a shears which close with increasing angular momentum and energy. Because of the geometry, the magnetic dipole moment vector has a net transverse component to the total angular momentum vector which breaks the isotropy of currents and leads to a rotation-like band. The magnetic dipole vector decreases in magnitude as the neutron and proton blades close increasing the total angular momentum. This leads to decreasing $B(M1)$ values [$B(M1) \propto |\mu_{\perp}|^2$] with increasing angular momentum, now confirmed in many MR bands [7].

In the mass 130–140 region, the low-$\Omega h_{11/2}$ proton orbitals lie near the Fermi surface favoring prolate shapes, whereas the high-$\Omega h_{11/2}$neutron orbitals lie near the Fermi surface and favor an oblate shape. The nuclear shape can, therefore, be stabilized at different specific values of gamma deformation. Because of the right combination of orbitals near the Fermi surface, several $\Delta I = 1$ bands have been observed in the mass 130–140 region and have been labeled as MR bands [6]. Recently, magnetic dipole bands in ^{141}Eu [8], ^{142}Gd [9],

^{134}Ce [10], and ^{136}Ce [11] have been interpreted as MR bands. The ^{137}Pr nucleus had been studied earlier by Xu *et al.* [12] and Dragulescu *et al.* [13] by using heavy-ion reactions. In the present work, we focus upon a partial level scheme of ^{137}Pr nuclide and conclusively identify and extend a $\Delta I = 1$ band as a strong candidate of MR band. The crossover $E2$ transitions in this band have been found for the first time. We also present calculations based on the TAC model which support our findings. A band-crossing of a 3qp and a 5qp band, both magnetic in nature, is suggested as an explanation of the observed back-bending in the $\Delta I = 1$ MR band.

II. EXPERIMENTAL DETAILS

High spin states in the odd proton ^{137}Pr nucleus were populated through the ^{122}Sn(^{19}F, $4n$) reaction at 80 MeV beam energy. The ^{19}F beam was delivered by the 15-UD Pelletron accelerator at the Inter-University Accelerator Center (formerly known as Nuclear Science Centre, New Delhi). A self-supporting enriched ^{122}Sn target of thickness 1.2 mg/cm^2 was used. γ-γ coincidences were collected with the eight Compton suppressed clover detector array (INGA). Four of the clovers were placed at 81° and rest of the four at 141° with respect to the beam direction. A total of about 6.3×10^8 γ-γ coincidences were collected in list mode during 15 shifts of the experiment. The efficiency and energy calibrations were carried out by using ^{133}Ba and ^{152}Eu radioactive sources. Data were sorted into 4K $\times$ 4K $E_{\gamma_1} - E_{\gamma_2}$ matrix after gain matching in the offline analysis by using the INGASORT [14] program. Gamma ray spectra were obtained by taking projections along one of the axes while putting gates on the other one. Typical sum gated gamma ray spectrum showing all the dipole transitions (marked by asterisk) in the $\Delta I = 1$ band of our interest are presented in Fig. 1(a). All the peaks (except three) in this figure have been identified and placed in the level scheme. Some of the strong peaks like 128, 149, 187, 198, 209, and 562 keV belong to the positive part of the level scheme. The 597 keV represents the connecting transition from negative to positive parity states [12,13]. Three of the peaks belong to ^{136}Pr and are very weak. We further show in Fig. 1(b), a spectrum gated on the 465 keV transition where all the three new dipole transitions of 507, 577, and 657 keV are present. We have further confirmed the placement of the new transitions by putting successively higher gates. The placement also fits in with the observed $E2$ transitions.

III. RESULTS

In the present paper, we focus upon the negative parity $\Delta I = 1$ band proposed earlier by Xu *et al.* [12]. A partial level scheme, constructed from our analysis and containing three band structures all of them having negative parity, is shown in Fig. 2. The lowest lying level shown in Fig. 2 was assumed to have a spin and parity of $5/2^+$ on the basis of earlier measurements [15]. Band 1 has been established up to the spin $(35/2^-)$, while the structure of band 3 is not so clear. The most prominent of these is a long $\Delta I = 1$ band (band 2). The relative intensities have been determined from the coincidence data

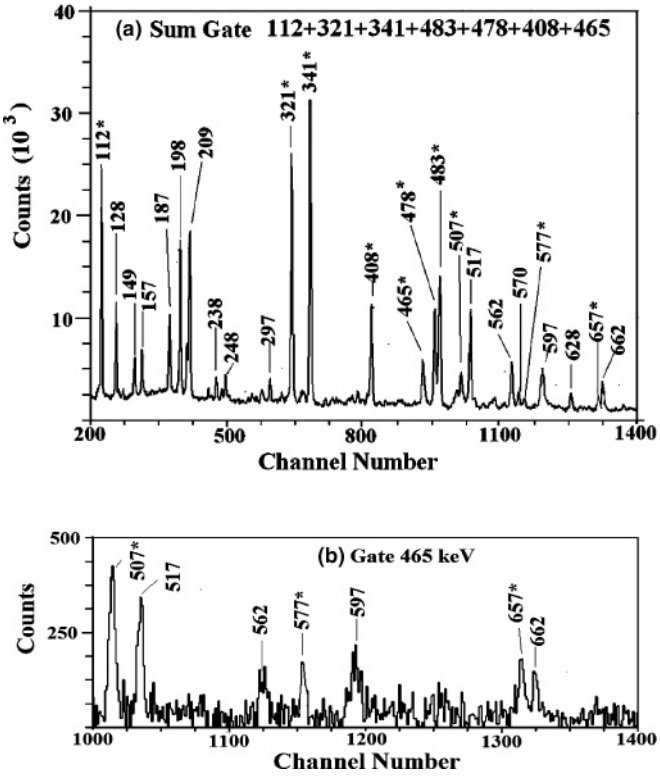

FIG. 1. (a) Sum gate spectrum showing the dipole transitions (marked by asterisks) in the $\Delta I = 1$ band (band 2). All the peaks have been accounted for as explained in the text. (b) Spectrum for a gate on 465 keV showing all the three higher lying dipole transitions.

in the 517 keV gate; intensities were normalized to 100 for the 517 keV transition. The multipolarities of transitions have been determined from linear polarization measurements and DCO ratios obtained from the spectra gated by the 517 keV $E2$ transition. Figure 2 also shows the presence of prominent $M1$ transitions up to the spin $41/2^-$ in agreement with the results reported by Xu *et al.* [12]. In addition we have extended the level scheme up to $47/2^-$ with the addition of three new transitions, namely, 507 keV, 577 keV, and 657 keV. These transitions are seen in the sum spectrum as shown in Fig. 1(a) and in the 465 keV gated spectrum shown in Fig. 1(b). Our measurements also show that 507, 577, and 657 keV gamma rays are in coincidence with each other. These measurements coupled with γ ray intensity measurement have established the placement of three γ rays above $41/2^-$ level in band 2 as shown in Fig. 2. The ordering of all the $M1$ transitions in band 2 has been further confirmed through the detection of crossover $E2$ transitions in band 2 for the first time. The crossover 433 keV $(29/2^- \rightarrow 25/2^-)$ transition is shown in the 483 + 478 keV gate in Fig. 3(a). The other crossover $E2$ transitions namely 819, 824, 873, 962, and 972 keV are shown in the 321 + 112 keV gate in Fig. 3(b). Finally the high energy 1084 keV and 1234 keV $E2$ transitions are shown in the 408 + 465 keV gate in Fig. 3(c). The 749 keV transition also shows up in the gate of 478 + 483 keV, not shown here. Similarly, the 662.5 keV $(31/2^-$ to $27/2^-)$ transition has been observed in the 774 keV gate, not shown here. Nine additional new transitions

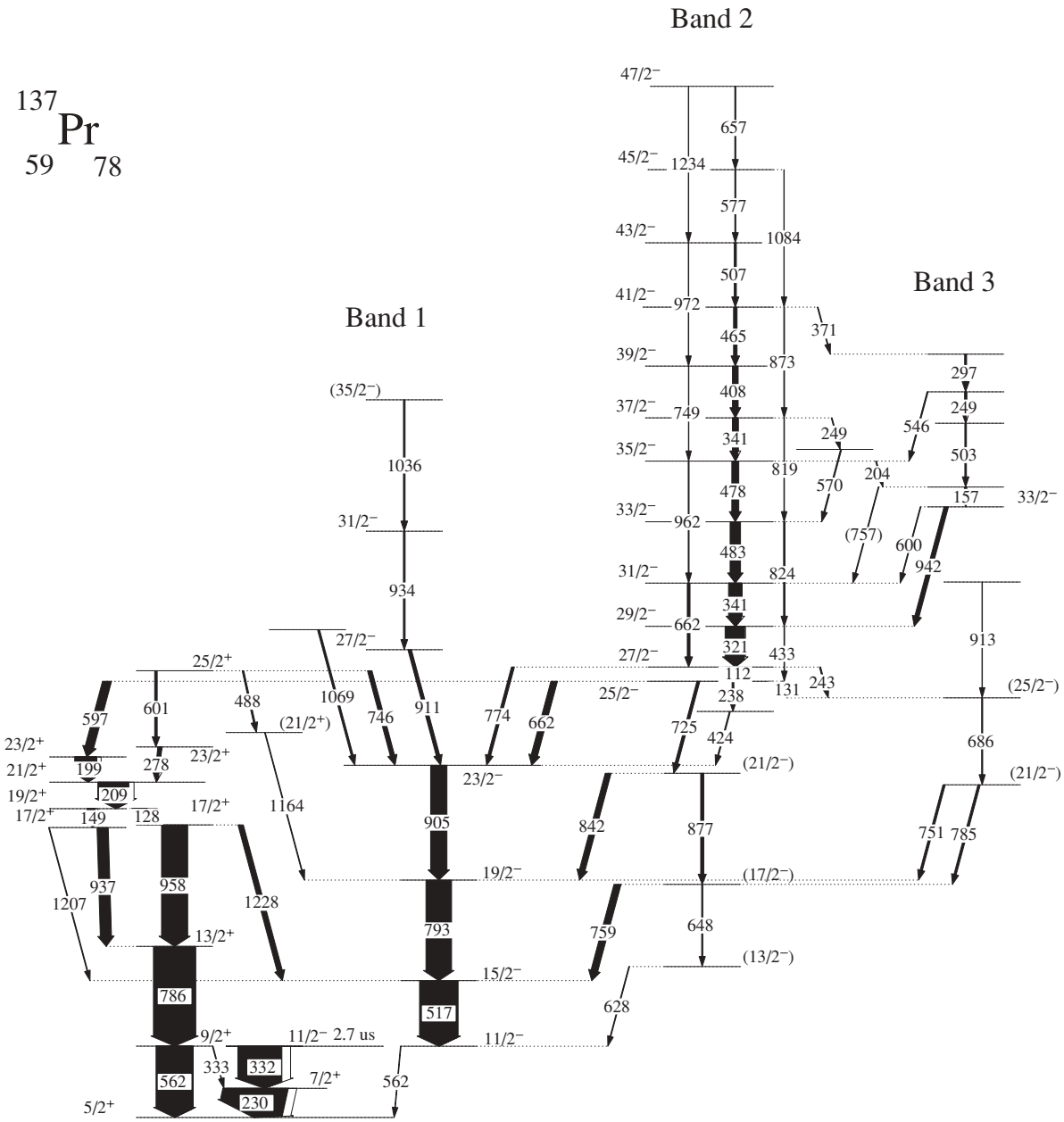

FIG. 2. Partial level scheme of ^{137}Pr as obtained from the present work.

observed are 238, 243, 249, 371, 424, 546, 570, 600, 757 which have been placed in the level scheme. The relative intensity measurements, DCO ratios and polarizations along with the earlier spin assignments for the lower lying states, have enabled us to make definite spin and parity assignments for the $\Delta I = 1$ band. The DCO ratio has been defined as

$$R_{\mathrm{DCO}} = \frac{I_{\gamma 1} \text{ at } 81^{\circ},\ \text{gated with } \gamma_2 \text{ at } 141^{\circ}}{I_{\gamma 1} \text{ at } 141^{\circ},\ \text{gated with } \gamma_2 \text{ at } 81^{\circ}}.$$

The values of R_{DCO} for most of the transitions are listed in Table I. The calculated DCO ratios of 0.5 and 1.0 are expected for stretched and pure transitions of multipole order 1 and 2, respectively, if the gate is set on an $\Delta I = 2$ transition (e.g., the 517 keV $E2$ transition); for values significantly different from 0.5 and 1.0, the transition is dipole + quadrupole (D + Q where D is dipole and Q is quadrupole transition) $\Delta I = 1$. Similarly, for DCO ratio $\approx$1.0, the transition is $\Delta I = 1$ stretched dipole if the gate is set on a $\Delta I = 1$ transition (e.g., 112 keV $M1$ transition). All the DCO ratios for a gate on 517 keV $E2$ transition, which could be calculated, are plotted in Fig. 4(a). It is evident from this figure that all the transitions in the $\Delta I = 1$ band have $M1$ nature as they lie around 0.5. The DCO ratio for 507.2 and 576.7 keV gamma could not be determined from a gate on 517 keV. Therefore, Fig. 4(b) shows the DCO ratios for a gate on 112 keV $M1$ transition, confirming the dipole nature of these transitions. While the $M1$ transitions

TABLE I. Energies, relative intensities, DCO ratios, polarization asymmetry data for transitions observed among the negative parity states of ^{137}Pr. The deduced multipolarities, $B(M1)/B(E2)$ values and the spin assignments are also listed. D stands for the dipole transitions and Q for the quadrupole transitions.

E_γ (KeV)	I_γ	DCO ratio with gate on 517γ, and 112γ (marked as $*$)	Δ_{IPDCO}	Multi-polarity	$B(M1)/B(E2)$ $(\mu_N/e\text{b})^2$	Assignment
			Band 1			
517.0(1)	100		+0.49(28)	$E2$		$15/2^- \rightarrow 11/2^-$
793.0(1)	66.8(21)	0.94(3)	+0.16(9)	$E2$		$19/2^- \rightarrow 15/2^-$
905.1(2)	42.7(25)	0.93(4)	+0.031(2)	$E2$		$23/2^- \rightarrow 19/2^-$
911.0(2)	9.0(6)	1.8 (1)	+0.38(15)	$(E2)$		$27/2^- \rightarrow 23/2^-$
934.7(3)	4.4(5)	1.2(2)				$31/2^- \rightarrow 27/2^-$
1036.6(4)	4.2(3)	.80(3)		$(E2)$		$(35/2^-) \rightarrow 31/2^-$
			Band 2			
111.9(2)	28.3(10)	0.55(1)	−0.04(2)	$M1$		$27/2^- \rightarrow 25/2^-$
321.0(1)	50.9(17)	0.51(1) 1.00(3)*	−0.06(2)	$M1$		$29/2^- \rightarrow 27/2^-$
341.5(1)	34.0(8)	0.52(1) 1.00(2)*	−0.19(7)	$M1$		$31/2^- \rightarrow 29/2^-$
483.4(1)	26.8(12)	0.56(1) 1.00(9)*	−0.10(5)	$M1$		$33/2^- \rightarrow 31/2^-$
478.0(1)	17.9(10)	0.52(2) 1.01(11)*	−0.06(1)	$M1$		$35/2^- \rightarrow 33/2^-$
341.4(1)	14.7(4)	0.51(3) 1.00(2)*		$M1$		$37/2^- \rightarrow 35/2^-$
408.4(1)	14.6(13)	0.51(4) 1.00(8)*	−0.04(2)	$M1$		$39/2^- \rightarrow 37/2^-$
465.5(1)	8.9(11)	0.49(5) 1.03(7)*	−0.03(2)	$M1$		$41/2^- \rightarrow 39/2^-$
507.2(2)	5.7(3)	0.96(10)*	−0.05(2)	$M1$		$43/2^- \rightarrow 41/2^-$
576.7(2)	2.4(1)	0.91(13)*	−0.06(1)	$M1$		$45/2^- \rightarrow 43/2^-$
657.4(2)	2.6(4)	0.70(22) 1.18(19)*	−0.15(12)	$M1$		$47/2^- \rightarrow 45/2^-$
432.6(4)	1.6(3)			$E2$	10.4(19)	$29/2^- \rightarrow 25/2^-$
824.1(4)	3.6(6)			$E2$	17.2(28)	$33/2^- \rightarrow 29/2^-$
819.4(4)	1.4(2)			$E2$	62.1(120)	$37/2^- \rightarrow 33/2^-$
872.3(4)	1.9(3)			$E2$	17.2(29)	$41/2^- \rightarrow 37/2^-$
1083.6(4)	1.0(2)			$E2$	12.8(27)	$45/2^- \rightarrow 41/2^-$
662.5(3)	7.1(17)			$E2$	10.5(23)	$31/2^- \rightarrow 27/2^-$
961.7(8)	2.3(4)			$E2$	41.2(74)	$35/2^- \rightarrow 31/2^-$
749.2(5)	1.0(3)			$E2$	33.3(88)	$39/2^- \rightarrow 35/2^-$
972.1(5)	1.1(2)			$E2$	18.5(32)	$43/2^- \rightarrow 39/2^-$
1233.7(4)	1.0(3)			$E2$	18.9(48)	$47/2^- \rightarrow 43/2^-$
			Band 3			
156.8(2)	4.8(3)	0.67(7)		(D+Q)		
502.8(2)	4.0(4)	0.50(7)	.007(4)	(E1)		
248.6(2)	5.0(5)	0.82(8)		(D+Q)		
297.2(2)	4.8(5)	0.67(3)		(D+Q)		
942.0(1)	11.2(10)	0.83(12)	0.1(3)	$E2$		$33/2^- \rightarrow 29/2^-$
			Other transitions from bands 2 and 3			
628.0(3)	2.0(1)					$(13/2^-) \rightarrow 11/2^-$
648.0(2)	2.99(1)		0.20(13)			$(17/2^- \rightarrow 13/2^-)$
758.6(2)	17.9(10)	0.45(6)		$(M1)$		$(17/2^-) \rightarrow 15/2^-$
785.0(3)	5.9(4)					$(21/2^- \rightarrow 17/2^-)$
876.6(2)	8.1(6)	0.81(8)				$(21/2^- \rightarrow 17/2^-)$
750.9(1)	5.8(5)	0.60(12)		$(E2)$		$(21/2^-) \rightarrow 19/2^-$
842.0(2)	14.9(15)	0.63(5)		$(M1)$		$(21/2^-) \rightarrow 19/2^-$
685.5(3)	2.8(3)	1.36(20)	+0.10(5)	$(E2)$		$(25/2^- \rightarrow 21/2^-)$
725.8(3)	7.5(5)	1.2(3)	+0.25(11)	$(E2)$		$25/2^- \rightarrow (21/2^-)$
424.0(2)	2.6(2)	0.78(15)	+0.24(9)	(E1)		
238.3(2)	4.2(6)	0.57(11)	+0.08(2)	E1		
131.0(3)	2.9(3)	1.03(24)		$(E2)$		$25/2^- \rightarrow (25/2^-)$
662.1(1)	16.6(2)	0.60(3)	−0.25(17)	$(M1)$		$25/2^- \rightarrow 23/2^-$
774.6(3)	7.5(7)	0.92(5)		$E2$		$27/2^- \rightarrow 23/2^-$
243.0(3)	2.9(2)					$27/2^- \rightarrow (25/2^-)$
913(1)	1.1(20)					
570.2(2)	2.8(1)					

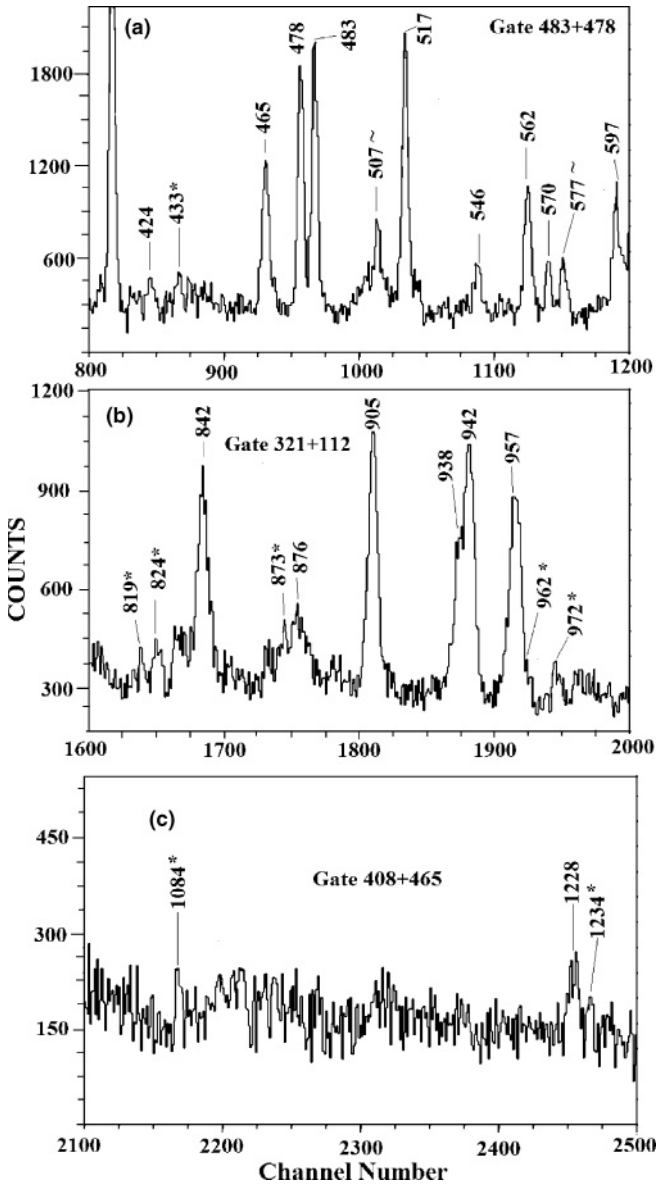

FIG. 3. (a) Sum gate (483 + 478) spectrum showing the $E2$ transitions marked by asterisks. Also shown are the new $M1$ transitions in the range of the graph. (b) and (c) Same as (a) but for the sum gates of (321 + 112) and (408 + 465) keV, respectively. All the other prominent peaks have been placed in the level scheme.

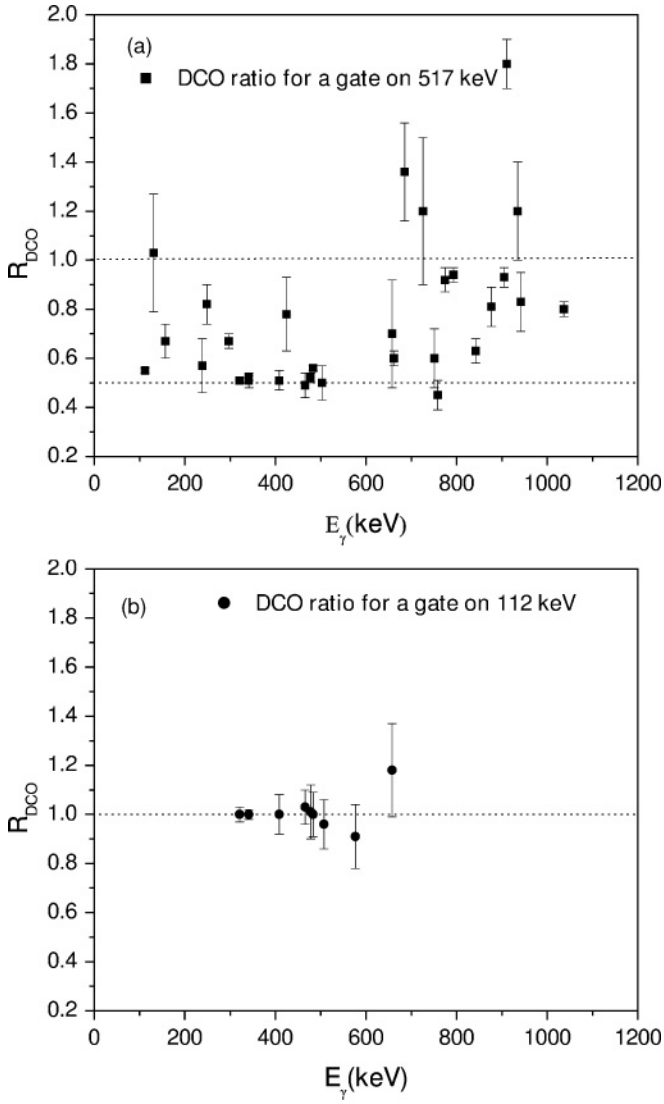

FIG. 4. DCO ratios for the transitions in the $\Delta I = 1$ band (band 2) and for few other transitions for gate on 517 keV $E2$ transition are shown in the upper block (a) and for a gate on 112 keV $M1$ transition in the lower block (b).

are very strong, very weak $E2$ crossover transitions have also been observed in the gated sum spectrum for the first time. The multipolarity of these transitions have been assigned on the basis of definite spin and parity assignments of the levels in the band 2. The relative intensities measured in the present work (Table I) match reasonably with those of Xu *et al*. [12] except for three transitions namely the 131.0, 725.8, 842.0 keV transitions which exhibit significantly lesser relative intensities in our measurements.

The linear polarization of the radiation can be determined through a difference between the number of Compton scattered gamma rays in a parallel reaction plane ($N_{||}$) and a perpendicular plane ($N_{\perp}$). A polarization matrix needs to be constructed from the data. From the projection spectrum, the number of $N_{||}$ counts and $N_{\perp}$ counts for a given γ ray can be obtained so that the asymmetry is given by

$$\Delta_{\mathrm{IPDCO}} = \frac{aN_{\perp} - N_{||}}{aN_{\perp} + N_{||}},$$

where a is a correction parameter; the value of a is almost 1. A negative value of Δ_{IPDCO} corresponds to magnetic nature of the transition whereas a positive value of Δ_{IPDCO} corresponds to electric nature of the transition. The results of our analysis are listed in Table I using the results of the table we have assigned spins and parities to higher lying levels as shown in Fig. 2.

The $B(M1)/B(E2)$ ratios have also been extracted from the data by using the relation

$$\frac{B(M1)}{B(E2)} = .697\frac{I(M1)E_{\gamma}^{5}(E2)}{I(E2)E_{\gamma}^{3}(M1)}(\mu_N/e\mathrm{b})^2,$$

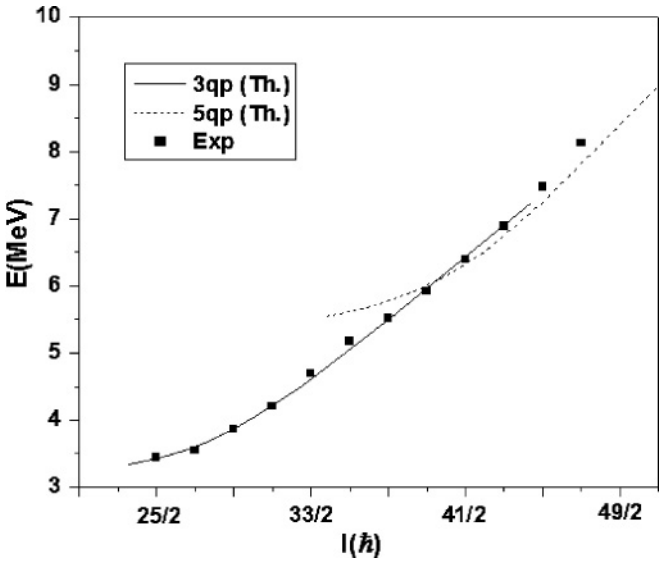

FIG. 5. A comparison of the measured energy E (MeV) vs spin I for the $\Delta I = 1$ band (band 2) with those calculated for the 3qp:$\{\pi h_{11/2} \otimes \nu(h_{11/2})^{-2}\}$ and the 5qp:$\{\pi h_{11/2}(g_{7/2})^2 \otimes \nu(h_{11/2})^{-2}\}$ configurations. A crossing may be seen in both the calculated as well as the measured values.

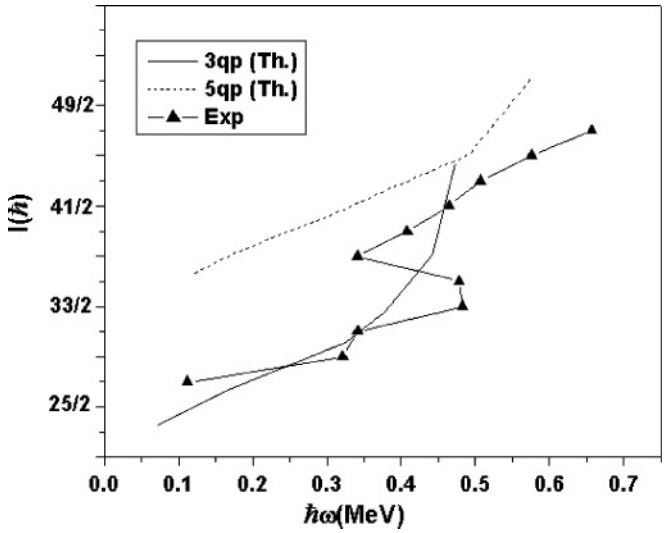

FIG. 6. A comparison of the experimental spin I vs $\hbar\omega$ for the $\Delta I = 1$ band (band 2) with the calculated results from the TAC model.

where E_γ is the gamma ray energy in MeV and $I_\gamma(M1)$ and $I_\gamma(E2)$ are the γ-ray relative intensities, and are listed in Table I. The mixing ratio parameter δ^2 is assumed to be negligible. For most of the $E2$ transitions which are very weak, we have used an average of the relative intensities obtained from sums of many gated spectra. These ratios are very large, much larger than those observed in the deformed nuclei. This is expected for magnetic rotation where $B(M1)$ values are large, due to the large magnetic moment component perpendicular to the total angular momentum, and the $B(E2)$ values are small due to the small quadrupole deformation.

IV. DISCUSSION

Band 1 is a negative parity band which was interpreted [12] as arising from a $h_{11/2}$ proton. The upbend at $\hbar\omega = 0.44$ MeV was suggested to arise from an alignment of two (second and third) $h_{11/2}$ protons. Cranked shell model calculations suggest a prolate nuclear shape with $\gamma = 0^\circ$. This is a reasonable interpretation of the band. Band 3 is quite irregular and spin parity assignments could not be made because of insufficient data. Further experimental measurements are necessary before any firm assignment may be made.

We now consider the interpretation of the $\Delta I = 1 M1$ band (band 2), which is the most prominent feature of the partial level scheme shown in Fig. 2. An interesting and important feature of the $\Delta I = 1$ band is the observation of a prominent back-bending in the experimental curve at $\hbar\omega = 0.48$ MeV as discussed later in the section.

The experimental observations have been compared with the detailed calculations based on the hybrid version of the tilted axis cranking (TAC) model [16,17]. This model proposed in [16] combines the best of the single particle potentials based on the Woods-Saxon and the modified oscillator potentials (Nilsson model). The Nilsson model with standard set of parameters does not work so well in $A = 130$ mass region. Therefore, the single particle energies of the spherical Woods-Saxon are taken and combined with the deformed part of the anisotropic oscillator. This approximation has the advantage of using a realistic flat bottom potential along with the coupling between the oscillator shells taken into account in a simple way. The pairing parameters were chosen as 80% of the odd-even mass difference, i.e., $\Delta_p = 1.048$ MeV and $\Delta_n = 0.65$ MeV. On the basis of the earlier studies [12] and comparison with neighboring nuclei, we have assigned a three-quasiparticle (3qp) configuration $\pi h_{11/2} \otimes \nu(h_{11/2})^{-2}$ to the observed negative parity $\Delta I = 1$ band. The Lund convention (ε_2, γ) for the shape parameters has been followed which gives oblate shape at $\gamma = 60^\circ$. The 3qp configuration yields a minimum in the total energy at a deformation of $\varepsilon_2 = 0.135$, $\varepsilon_4 = 0.009$, $\gamma = 58^\circ$ with an average tilt angle $\theta \sim 25^\circ$ [18]. It was, however, found necessary that a five-quasiparticle (5qp) configuration $\pi h_{11/2}(g_{7/2})^2 \otimes \nu(h_{11/2})^{-2}$ be introduced at higher spins to explain the back-bending feature. For the 5qp configuration, a minimization in energy gives a deformation of $\varepsilon_2 = 0.126$, $\varepsilon_4 = 0.0$, $\gamma = 58^\circ$ with an average tilt angle $\theta \sim 26^\circ$ [19], which is nearly the same as that of the 3qp configuration. However, this minimum lies about 2.2 MeV higher than the 3qp minimum. For a better comparison of calculated results with experimental data, the TAC calculations have been done for both the 3qp configuration and the 5qp configuration with an attenuation factor $\eta = 0.6$ instead of the commonly used value of $\eta = 0.7$. Here η is a factor by which the free nucleon magnetic moment is attenuated.

Figure 5 compares the E vs I plots for the 3qp configuration and the 5qp configuration with the measured values. The TAC calculations for the 3qp and 5qp configuration show

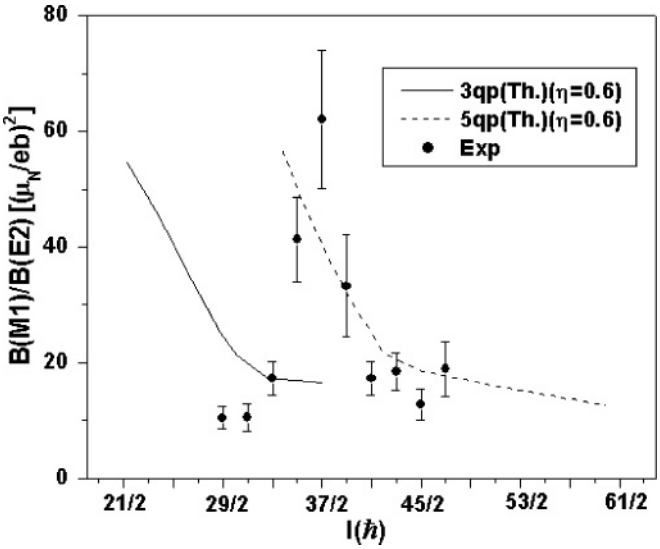

FIG. 7. The experimental values of $B(M1)/B(E2)$ vs spin I for the $\Delta I = 1$ band (band 2) compared with the TAC calculations.

a band-crossing near $I(\hbar) \approx 39/2$. A careful look at the experimental data reveals that there is indeed a crossing of bands around $I(\hbar) \approx 35/2$, where a point of inflexion is seen. It may, however, be seen that the experimentally measured values at lower spins corresponds to the 3qp results from the TAC calculations; however they do not cover the entire $\Delta I = 1$ band. The 5 qp results can be taken to reproduce the measured values after $I(\hbar) \approx 39/2$. The experimental data are, therefore, fairly consistent with the interpretation that a band-crossing is indeed present and the lower part of the $\Delta I = 1$ band corresponds to the 3qp configuration while the upper part corresponds to the 5qp configuration. The calculated 5qp band is, however, shifted upwards in energy and, angular momentum by two units.

This band-crossing becomes evident as it leads to a back-bending in the I vs $\hbar\omega$ plot shown in Fig 6. It is not possible to explain the back-bending by taking the 3qp configuration alone or, the 5qp configuration alone. The calculated 3qp band is observed to be close to the experimental data up to $\hbar\omega = 0.3$ MeV; it exhibits an up-bend afterwards. The lower portion of the calculated 5qp band is observed to be parallel to the experimental curve (just after the backbend). The discrepancy between the calculated and the experimental results of the 5qp band as noted above (discussion of Fig. 5), causes a discrepancy of two units here also. This appears to be a result of poor normalization in calculated values. The general trends, however, are explained well and will not change even after a better normalization of the 3qp and 5qp energies is done. It may be noted that the 5qp band also exhibits a small up-bend at higher spins. The experimental curve also exhibits a slight up-bend but not such a drastic one as seen in the calculated 5qp band. The calculated 5qp band, therefore, deviates more from the measured values at higher spins. However, there is no way in which a 3qp band alone can explain the observed behavior. Hence, the back-bending observed at $\hbar\omega = 0.48$ MeV appears to be a result of the crossing of the 3qp band with the 5qp band.

Figure 7 shows a comparison of the experimental $B(M1)/B(E2)$ ratio with the calculated 3qp and 5qp configuration at an attenuation factor $\eta = 0.6$. The interpretation in terms of band-crossing presented above is quite consistent with the behavior of the $B(M1)/B(E2)$ ratio shown in Fig. 7. The measured ratio at lower spins increases with increase in spin up to $I = 37/2$, while at higher spins the ratio decreases with spin. In the lower spin region, the $B(M1)/B(E2)$ ratio at $I = 29/2$ to $I = 31/2$ lies close the 3qp calculated values, whereas at $I = 37/2$ and above the measured ratio lies close to the 5qp results. We, therefore, find that the band crossing of a 3qp band with a 5qp band having an extra aligned pair of $g_{7/2}$ protons, leads to a larger value of $B(M1)/B(E2)$. A similar situation is observed in ^{108}Cd [20] and ^{112}Sb [21] where the $B(M1)/B(E2)$ increases and then decreases; the structure of band is described in terms of two different configurations before and after the band-crossing due to $(\upsilon h_{11/2})^2$ alignment. In the present case, the values of $B(M1)/B(E2)$ at 35/2 lies in the transition region where the two bands mix with each other. The sudden rise at 37/2 is the point where the 5qp configuration $\pi h_{11/2}(g_{7/2})^2 \otimes \nu(h_{11/2})^{-2}$ takes over the band. This is reminiscent of the interpretation in terms of the reopening of blades at the band-crossing in the case of ^{197}Pb [22]. The theoretically calculated $B(M1)$ values (not shown in the paper) also show a decreasing trend with the increasing frequency for both the 3qp and 5qp configuration as expected for magnetic rotation. We, therefore, suggest that the lower part (corresponding to 3qp) as well as the upper part (corresponding to 5qp) represent magnetic rotation bands and what we are observing is a crossing of the two.

In conclusion, a $\Delta I = 1$ band has been extended to a spin of $47/2^-$ with the addition of three new transitions; the $M1$ nature of the band has been established by polarization measurements. In addition, very weak crossover $E2$ transitions have also been identified. The band appears to arise from the crossing of a 3qp $(\pi h_{11/2} \otimes \nu(h_{11/2})^{-2})$ and a 5qp $[\pi h_{11/2}(g_{7/2})^2 \otimes \nu(h_{11/2})^{-2}]$ configuration, which leads to a back-bending. The $B(M1)/B(E2)$ values obtained from the measurements show a behaviour which suggests a crossing of two magnetic rotation bands based on these configurations. Comparison of the theoretical calculations based on the TAC model with the measured values also supports an interpretation of magnetic rotation for both the configurations.

ACKNOWLEDGMENTS

The authors would like to thank all the participants of the joint national effort to set up the Clover Array (INGA) at the Inter-University Accelerator Centre (formerly known as Nuclear Science Centre), New Delhi. The help of the accelerator staff is gratefully acknowledged. Financial support from the Department of Science and Technology (Government of India), C.S.I.R. (India), I.A.E.A. (Vienna) at Roorkee, and Department of Atomic Energy (Government of India) at Amritsar is also gratefully acknowledged.

[1] H. Hübel, Prog. Part. Nucl. Phys. **54**, 1 (2005), and references therein.
[2] S. Frauendorf, Rev. Mod. Phys. **73**, 463 (2001).
[3] L. Funke, J. Doring, P. Kemnitz, E. Will, G. Winter, A. Johnson, L. Hildingsson, and Th. Lindblad, Nucl. Phys. **A455**, 206 (1986).
[4] S. S. Malik, P. Agarwal, and A. K. Jain, Nucl. Phys. **A732**, 13 (2004).
[5] R. M. Clark *et al*., Phys. Lett. **B275**, 247 (1992).
[6] Amita, A. K. Jain, and B. Singh, At. Data Nucl. Data Tables **74**, 283 (2000); http://www.nndc.bnl.gov/publications/preprints/mag-dip-rot-bands.pdf (2006).
[7] R. M. Clark *et al*., Phys. Lett. **B440**, 251 (1998).
[8] E. O. Podsvirova *et al*., Eur. Phys. J. A **21**, 1 (2004).
[9] A. A. Pasternak *et al*. , Eur. Phys. J. A **23**, 191 (2005).
[10] S. Lakshmi, H. C. Jain, P. K. Joshi, A. K. Jain, and S. S. Malik, Phys. Rev. C **69**, 014319 (2004).
[11] S. Lakshmi, H. C. Jain, P. K. Joshi, Amita, P. Agarwal, A. K. Jain, and S. S. Malik, Phys. Rev. C **66**, 041303(R) (2002).
[12] N. Xu, C. W. Beausang, R. Ma, E. S. Paul, W. F. Piel, Jr., D. B. Fossan, and L. Hildingsson, Phys. Rev. C **39**, 1799 (1989).
[13] E. Dragulescu *et al*., Nucl. Phys. **A548**, 435 (1992).
[14] R. K. Bhowmik, IUAC (private communication).
[15] H. Klewe-Nebenius, D. Habs, K. Wisshak, H. Faust, G. Nowicki, S. Goring, H. Rebel, G. Schatz, and M. Schwall, Nucl. Phys. **A240**, 137 (1975).
[16] V. I. Dimitrov, F. Donau, and S. G. Frauendorf, Phys. Rev. C **62**, 024315 (2000).
[17] Amita, A. K. Jain, V. I. Dimitrov, and S. G. Frauendorf, Phys. Rev. C **64**, 034308 (2001).
[18] P. Agarwal *et al*., *Proceedings of DAE-BRNS Symposium on Nuclear Physics (India)* **B46**, 36 (2003).
[19] P. Agarwal *et al*., *Proceedings of DAE-BRNS Symposium on Nuclear Physics (India)* **B47**, 38 (2004).
[20] N. S. Kelsall *et al*., Phys. Rev. C **61**, 011301(R) (2000).
[21] G. J. Lane *et al*., Phys. Rev. C **58**, 127 (1998).
[22] J. R. Cooper *et al*., Phys. Rev. Lett. **87**, 132503 (2001).